Study of iron-containing carbon-supported catalysts for oxidative decomposition of hydrogen sulfide: the activity—structure relationship

Yu. V. Maksimov,[a] M. V. Tsodikov,[b]* M. A. Perederii,[c] I. P. Suzdalev,[a] A. I. Nekhaev,[b] V. T. Popov,[b] and O. V. Bukhtenko[b]*

[a]*N. N. Semenov Institute of Chemical Physics, Russian Academy of Sciences, 4 ul. Kosygina, 117977 Moscow, Russian Federation. Fax: 007 (095) 938 2156*

[b]*A. V. Topchiev Institute of Petrochemical Synthesis, Russian Academy of Sciences, 29 Leninsky prosp., 117912 Moscow, Russian Federation. Fax: 007 (095) 230 2224*

[c]*Institute of Fossil Fuel, 29 Leninsky prosp., 117910 Moscow, Russian Federation. Fax: 007 (095) 230 2134*

Clusters of nonstoichiometric magnetite $Fe_3O_{4+\delta}$ and pyrrhotite $Fe_{1-c}S$ were shown to be the active structures of iron-containing carbon-supported catalysts for oxidative decomposition of hydrogen sulfide. A model of the surface active centers is discussed in terms of the anion vacancies participating in the reaction.

Key words: iron-containing catalysts, carbon supports; hydrogen sulfide, clusters, nonstoichiometric spinel, pyrrhotite, anion vacancies.

Catalytic processing of hydrogen sulfide producing elemental sulfur is of great importance to solve the environmental problem of neutralization of toxic wastes from plants which consume and process natural energy sources: gas, petroleum, and coal. Previously,[1] supported catalysts based on transition metals of VI—VIII groups which are capable of decomposing H_2S into elemental sulfur in the presence of CO_2 and O_2 as oxidants were studied. The activity of these catalysts was enhanced by their preactivation during thermal decomposition of light hydrocarbons at 773—873 K.[2] Metal-containing residues from hydrogenation of brown coal, whose production is complicated and power-consuming, were used as efficient catalysts of hydrogen sulfide decomposition.[3]

In this work, the relationship between the structure and activity of iron-containing catalysts of oxidative decomposition of H_2S supported on spherical carbon supports of different porosity was studied. The effect of the products of thermal decomposition of heptane on the structure and catalytic properties of the supported systems was investigated.

Experimental

Preparation of iron-containing catalysts. Two types of spherical carbon supports, **1** and **2**, with a granule diameter of 2—3 mm were used; they were obtained by preliminary grinding of coal, granulation, and subsequent carbonization and activation of the granules.[4] Table 1 presents the parameters of the pore structure and the composition of the mineral component of supports **1** and **2**. The iron-containing catalysts were obtained by impregnation of these supports with a solution of

Table 1. Characterization of the pore structure and composition of the mineral component of supports **1** and **2**

Parameter	**1**	**2**
$V_\Sigma/cm^3\ g^{-1}$	0.54	0.67
$V_{micro}/cm^3\ g^{-1}$	0.03	0.28
$V_{meso}/cm^3\ g^{-1}$	0.02	0.06
$V_{macro}/cm^3\ g^{-1}$	0.49	0.34
$s_{sp}/m^2\ g^{-1}$	42	732
Composition of the mineral component (%):		
SiO_2	4.07	6.90
CaO	0.93	1.61
MgO	0.44	0.71
Al_2O_3	1.89	3.26
Fe_2O_3	1.31	2.33
K_2SO_3	0.63	1.03
K_2O	0.13	0.31
Na_2O	0.25	0.40
P_2O_5	0.09	0.15
Ash content (%)	9.8	16.7

Note. V_Σ is the total pore volume; V_{micro}, V_{meso} and V_{macro} is the volume of micropores, mesopores, and macropores, respectively; s_{sp} is the specific surface area.

Translated from *Izvestiya Akademii Nauk. Seriya Khimicheskaya*, No. 1, pp. 86—90, January, 1997.

1066-5285/97/4601-0081 $18.00

iron acetylacetonate $Fe(acac)_3$; the Fe content in each sample was 2 wt.%. After deposition of iron, the samples were dried in air, calcined at 773 K in nitrogen, and activated in a flow reactor in heptane vapor medium at 773—873 K. In order to study the effect of inorganic ash impurities in the coal on the catalytic properties, support **1** was decalcified by HCl.[5]

Catalytic testing. The catalysts were tested in a flow glass reactor in the temperature range of 473—523 K. A mixture of air with 5 vol.% H_2S was passed through a fixed bed of the catalyst (~5 cm^3) with a space velocity of 2000 h^{-1} for 1 h. To determine the amount of unconverted H_2S, the reaction mixture was passed through a 10% solution of $Cd(MeCOO)_2$; the CdS precipitated was dried in a vacuum and weighed. The total productivity of a catalyst was evaluated by two parameters: H_2S conversion and reduced sulfur capacity (S) which characterizes the total amount of sulfur produced per 1 g of catalyst per 1 h. Regeneration and activation of the catalyst were carried out by thermal decomposition of heptane in a flow reactor at 773—873 K.

Investigation techniques. The X-ray diffractograms of the samples were recorded on a DRON-3M setup with filtered Cu-Kα radiation. The phases were identified by a comparison of the found interplanar distances with the known values.[6] The Moessbauer spectra were recorded at 77—300 K on an installation of the electrodynamic type with a ^{57}Co in chromium source. The isomeric shifts (IS) were calculated relative to α-Fe. The spectra were processed using standard programs under the assumption of a Lorentz line shape.[7] The pore structure of the supports and catalysts was studied on a vacuum adsorption-weight setup equipped with a Mack-Benn balance.[8] The specific surface area of the samples was determined by low-temperature adsorption of nitrogen in a volumetric adsorption installation.[9] The elemental composition of the samples was determined by the atomic-adsorption method on a Perkin-Elmer spectrometer.

Results and Discussion

Catalytic properties. When a mixture of hydrogen sulfide with air is passed through a layer of the catalyst, a significant fraction of H_2S decomposes, producing elemental sulfur. Table 2 presents the data on H_2S conversion in the presence of carbon supports **1** and **2** (samples *1* and *5*), decalcified support **1** (sample *2*), and iron-containing supported catalysts after different treatments (samples *3*, *4*, *6*, *7*, and *8*). It is seen that despite the considerable difference (nearly by one order of magnitude) in the micropore volumes of supports **1** and **2**, the carbon supports that were not treated with iron compounds exhibit significant and practically the same overall activity (for samples *1* and *5*, the H_2S conversion is ~60%). After removal of the ash components from the coal, H_2S conversion decreases to ~20% (sample *2*). Thus, the active sites initiating decomposition of hydrogen sulfide are present in the starting carbon supports, and their amount decreases after decalcification. After deposition of the $Fe(acac)_3$ complex on starting supports **1** and **2** and activation in a nitrogen atmosphere at 773 K (samples *3* and *6*) or successively in nitrogen at 773 K and in heptane vapor at 823 K (samples *4* and *7*), H_2S conversion increases to 83.3 and 94.3% or to 95.0 and 100%, respectively. During prolonged experiments on oxidative decomposition of H_2S, the iron-containing catalysts on macroporous (**1**) and microporous (**2**) carbon supports displayed different activity and stability. Thus, whereas the starting supports and iron-containing catalysts are comparable in their initial activity, the overall productivity of the catalyst on the microporous support **2** remains relatively high after a number of "catalysis—regeneration" cycles, unlike the catalyst on the macroporous support which is deactivated to a significant extent. In fact, after five regeneration cycles, the sulfur capacity, S, decreases for support **2** from 2.34 g S (g Cat h)$^{-1}$ (sample *7*) to 1.56 g S (g Cat h)$^{-1}$ (sample *8*), whereas for macroporous support **1**, $S \approx$ 0.28 g S (g Cat h)$^{-1}$ after only two regeneration cycles.

Table 2. Overall conversion of H_2S on iron-containing catalysts **1** and **2**

Sample	Support	Reagent for deposition	Treatment	Conversion of H_2S (%)
1	**1**	—	—	61.2
2	**1**	—	HCl	20.0
3	**1**	$Fe(acac)_3$	N_2 (773 K)	83.3
4	**1**	$Fe(acac)_3$	N_2 (773 K) + heptane (~823 K)	94.3
5	**2**	—	—	57.3
6	**2**	$Fe(acac)_3$	N_2 (773 K)	95.0
7	**2**	$Fe(acac)_3$	N_2 (773 K) + heptane (~823 K)	100.0
8	**2**	$Fe(acac)_3$	5 regeneration cycles	~70

The structure of the catalysts. In a typical Moessbauer spectrum of undoped carbon **1** or **2**, there are two sextets of magnetic hyperfine structure (HFS) due to the A and B positions of Fe atoms in the magnetically ordered clusters of nonstoichiometric magnetite $Fe_3O_{4+\delta}$ (Fig. 1, *a*); the average size (d) of the magnetic clusters is within ~5—7 nm. In addition to the lines of magnetic HFS, doublets caused by paramagnetic (at 300 K) high-spin ions Fe^{3+} and Fe^{2+} are present in the spectrum in Fig. 1, *a*. Approximately half of the signal from Fe^{3+} paramagnetic ions with parameters IS = 0.30 mm s^{-1} and quadrupole splitting (QS) equal to 0.68 mm s^{-1} most likely concerns superparamagnetic clusters of the $Fe_3O_{4+\delta}$ spinel with sizes of $d \approx 3$—5 nm.[10] Another half of the signal from Fe^{3+} ions along with the doublet from Fe^{2+} ions (IS = 0.92 mm s^{-1}, QS = 1.07 mm s^{-1}) can characterize the layered structure of the silicate.[11] Thus, in the ilvaite-type structure of $CaFe^{II}_2Fe^{III}[Si_2O_8(OH)]$, two mixed-charge states of the iron ions are present, which do not participate in electron-exchange processes at 300 K, and their parameters are close to those presented in Table 3. The X-ray diffraction data confirm the formation of spinel clusters which are characterized by broadened reflections with d/n = 0.28, 0.24, 0.25, and 0.21 nm.

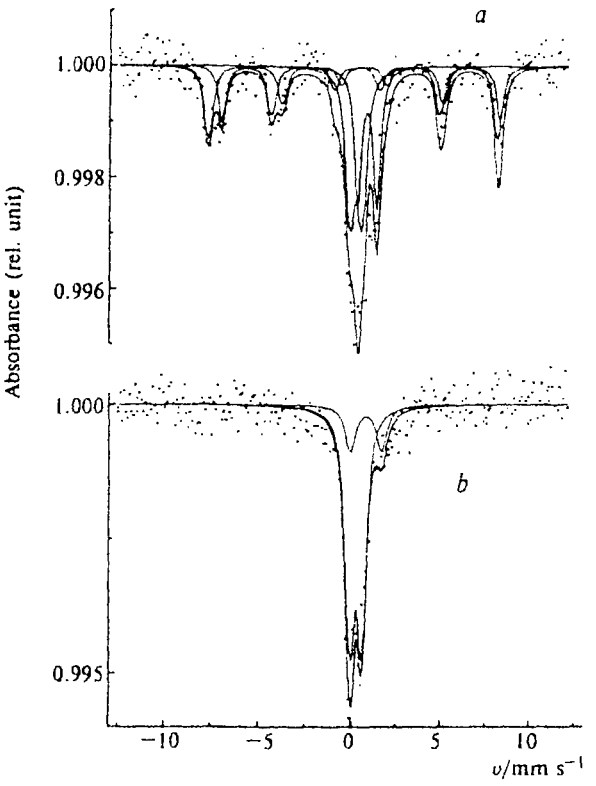

Fig. 1. Moessbauer spectrum of starting carbon support 1 at 300 K (*a*) and after treatment of support 1 by hydrochloric acid (*b*).

In the Moessbauer spectrum of the decalcified support (see Fig. 1, *b*), signals from comparatively large clusters of a spinel are virtually absent. At the same time, the doublets from Fe^{3+} and Fe^{2+} ions, entering the composition of smaller supermagnetic clusters of the $Fe_3O_{4+\delta}$ spinel and possibly the silicate, are observed. Thus, the largest clusters of nonstoichiometric magnetite react with the acid and are removed from the surface of the support. The smaller clusters of spinel and layered silicate remain in the structure of the support and do not interact with the acid, apparently due to steric hindrances.

The Moessbauer spectra of the carbon supports after deposition of the $Fe(acac)_3$ complex on their surface and activation are qualitatively similar to the spectrum of the starting support. However, the resonance absorption of the supported samples increases by several times. Hence, interaction of $Fe(acac)_3$ with the support is accompanied by exchange reactions of the ligands with the surface hydroxyl coverage resulting in destruction of the complex and formation of clusters of a complex oxide (spinel) that are isostructural to the natural forms of iron in carbon (see Table 3, samples *3* and *6*). The action of the products of thermal degradation of heptane at 773—873 K considerably changes the nature of the iron-containing structures. As follows from the data in Table 3 (samples *4* and *7*), a large fraction of the $Fe_3O_{4+\delta}$ clusters is reduced to metal and stoichiometric carbide Fe_3C. The X-ray diffraction data also give evidence of the formation of large clusters of iron metal and stoichiometric carbide which are characterized by the reflections with d/n = 0.267, 0.232, 0.212, 0.201, and 0.197 nm. It is noteworthy that during oxidative decomposition of H_2S, a fraction of the iron metal is repeatedly oxidized to nonstoichiometric magnetite $Fe_3O_{4+\delta}$.

The structural and catalytic data obtained make it possible to conclude that the nonstoichiometric spinel $Fe_3O_{4+\delta}$ which is present in the starting carbon support and the iron-containing catalyst is the basic structure in

Table 3. Parameters of the Moessbauer spectra of the iron-containing structures in catalysts 1 and 2 at 300 K

Sample	Fe compounds	IS (mm s^{-1}, ±0.03)	QS (mm s^{-1}, ±0.03)	B_{in} /T (±1)	Relative content (±0.05)
1	Magnetic:				
	$Fe_3O_{4+\delta}$ (A)	0.30	−0.02	49.7	0.26
	$Fe_3O_{4+\delta}$ (B)	0.73	−0	47.7	0.21
	Paramagnetic:				
	Fe^{3+}	0.30	0.68	—	0.29
	Fe^{2+}	0.92	1.07	—	0.25
2	Paramagnetic:				
	Fe^{3+}	0.29	0.66	—	0.79
	Fe^{2+}	0.87	1.74	—	0.21
3, *6*	Magnetic:				
	$Fe_3O_{4+\delta}$ (A)	0.34	−0.02	48.9	0.18
	$Fe_3O_{4+\delta}$ (B)	0.78	−0	45.6	0.30
	Paramagnetic:				
	Fe^{3+}	0.28	0.68	—	0.33
	Fe^{2+}	0.78	1.27	—	0.18
4, *7*	Magnetic:				
	α-Fe	0.05	0	32.9	0.14
	Fe_3C	0.24	0.02	20.8	0.38
	Paramagnetic:				
	Fe^{3+}	0.29	0.78	—	0.30
	Fe^{2+}	1.12	2.05	—	0.18
8	Magnetic:				
	α-Fe	0.02	0	33.0	0.24
	$Fe_{1-x}S$	0.73	0.02	30.8	0.18
	$Fe_3O_{4+\delta}$ (A)	0.34	−0.02	46.9	0.02
	$Fe_3O_{4+\delta}$ (B)	0.78	−0	44.6	0.03
	Paramagnetic:				
	Fe^{3+}	0.30	0.68	—	0.29
	Fe^{2+}	1.07	0.60	—	0.24

Note. B_{in} is the inner field on the Fe nucleus; for the composition of samples, see Table 2.

formation of surface active sites. This is confirmed by the drop in the catalytic activity of the demineralized support, from which a significant fraction of the clusters of the $Fe_3O_{4+\delta}$ spinel is removed. The increase in the catalytic activity after deposition of $Fe(acac)_3$ is due to the increasing content of active phase formed during destruction of the complex. The substantial increase in the activity after treatment with heptane is due to the appearance of reduced species of iron and carbide. As the clusters formed are very reactive, they are rapidly oxidized to the nonstoichiometric spinel that participates in the formation of surface active sites. The cluster species of Fe_3C carbide can play the role of a structural promoter which enlarges the interphase boundaries in the catalyst, thus favoring accessibility of the active sites of the surface for the molecules of reagents.

Model of the active structure. The activity of nonstoichiometric magnetite in oxidative decomposition of H_2S can be explained by the presence of anionic vacancies and labile oxygen O_s on the surface of the oxide. The building block of the $Fe_3O_{4+\delta}$ reversed spinel which is intermediate between magnetite (Fe_3O_4) and maghemite (γ-Fe_2O_3) has the following formula:[12]

$$Fe_A^{3+}[(Fe^{2+}_{1-3\delta}Fe^{3+}_{1-3\delta})Fe^{3+}_{5\delta}\square_{\delta}]_BO_4^{2-},$$

where A and B are the tetrahedral and octahedral positions of the iron atoms; $\square$ is a cationic vacancy, $(Fe^{2+}_{1-3\delta}Fe^{3+}_{1-3\delta})$ are pairs of cations in the B sublattice with the bridging O atom participating in double exchange (according to Wervey); δ is a parameter of nonstoichiometry varying from 0 (magnetite) to 1/3 (maghemite). The formation of each new cationic vacancy in the B sublattice during oxidation eliminates five Fe^{3+} ions from coupling exchange and results particularly in the formation of surface Fe—O_s groups with the terminal rather than the bridging O atom.

By analogy with the phenomena of photoreduction and photocatalysis which were studied previously[13,14] for vanadyl, chromyl, and molybdenyl octahedral complexes of transition metals, thermal activation of the surface oxygen of terminal groups in the nonstoichiometric magnetite can be treated as thermal electronic exitation of the Fe—O_s bond with intermediate formation of a radical-anionic oxygen species.[15] The shift in the electron density from the O atom to the metal and the high extent of covalent bonding causes high mobility of the terminal oxygen. In particular, when an O atom is removed from the lattice during activation, surface anionic vacancies (V_s) arise which can be considered as active sites of oxidative decomposition of H_2S:

$$Fe{-}O_s \rightarrow V_s + 1/2\ O_2 \qquad (1)$$

$$H_2S + V_s \rightarrow Fe{-}S_s + H_2. \qquad (2)$$

The appearance of sulfide fragments Fe—S_s on the surface of the spinel is an intermediate step in the formation of the highest sulfides, in particular $Fe_{1-x}S$, pyrrhotite, and elemental sulfur. When the performance of the catalyst is prolonged, *i.e.*, after a few cycles of regeneration, the fraction of nonstoichiometric pyrrhotite increases at the expense of the spinel (see Tables 2 and 3, sample *8*). The formation of pyrrhotites slightly decreases the overall activity of the catalysts. Thus, the sulfur capacity of catalyst 2 is lowered to ~1.56 g S (g Cat h)$^{-1}$, and this corresponds to average conversion of H_2S of ~70%. Nonstoichiometric pyrrhotite is known to be a catalyst of hydrogenation of high-sulfur petroleum and sulfur-containing coal.[16,17] The nonstoichiometric defects of pyrrhotites seem to serve as surface active sites that coordinate sulfur ions. The capability of sulfur to form oligomeric clusters can prevent formation of stoichiometric iron sulfides.

Thus, the active structures of iron-containing catalysts on carbon supports for hydrogen sulfide decomposition are clusters of nonstoichiometric spinel $Fe_3O_{4+\delta}$, which are present in the ash component of the support. The fraction of such clusters increases when the support is modified by $Fe(acac)_3$, apparently due to epitaxial growth of the active phase on the already existing clusters of the spinel. The clusters of nonstoichiometric pyrrhotite $Fe_{1-x}S$ formed are also catalytically active in decomposition of hydrogen sulfide. The high defectness and stability of the catalysts on the microporous support is due to the presence of $Fe_3O_{4+\delta}$ nanoclusters microencapsulated in the pore mouths. The formation of larger particles of the spinel on the macroporous support results in a decrease in the mobility of the terminal oxygen and a drop in the overall activity of the catalyst.

This work was financially supported by the Russian Foundation for Basic Research (Project No. 94-03-08081).

References

1. E. Richter, *Catal. Today*, 1990, **7**, 93.
2. USSR Pat. 1692031, 1988 (in Russian).
3. USSR Pat. 1761236, 1992 (in Russian).
4. M. A. Perederii and V. N. Khotuleva, *Trudy IGI* [*Works of IGI*], 1986, 53 (in Russian).
5. M. A. Perederii, S. I. Surinova, and V. N. Khotuleva, *Khim. Tverd. Tela* [*Solid State Chemistry*], 1983, 3, 101 (in Russian).
6. *Powder Diffraction File*, JCCAPDM, Philadelphia, USA, 1964.
7. Yu. V. Maksimov, I. P. Suzdalev, T. I. Khomenko, and A. A. Kadushin, *Hyperfine Interaction*, 1990, 57, 1987.
8. N. N. Dubinin, in *Adsorbtsiya i poristost'* [*Adsorption and Porosity*], Izd. Akad. Khimzashchity, Moscow, 1972, 18 (in Russian).
9. *Metody issledovaniya v tekhnicheskoi adsorbtsii* [*Investigation Methods in Technical Adsorption*], Ed. N. S. Torocheshnikov, Izd. MKhTI, Moscow, 1977, 80 (in Russian).
10. M. V. Tsodikov, V. Ya. Kugel, Yu. V. Maksimov, O. G. Ellert, V. M. Shcherbakov, and O. V. Bukhtenko, *J. Catal.*, 1994, **148**, 113.

11. H. Eckert, in *Modern Inorganic Chemistry*, 2, Ed. G. J. Long, Plenum Press, New York, 1987, 164.
12. O. V. Morozova, Yu. V. Maksimov, D. P. Shashkin, and O. V. Krylov, *Appl. Catal.*, 1991, **78**, 227.
13. V. B. Kazansky, *Proc. 6th Intern. Congr. on Catalysis*, Bath. Pitman Press, London, 1976, **1**, 50.
14. V. B. Kazansky, A. N. Pershin, and B. N. Shelimov, *Proc. 7th Intern. Congr. on Catalysis*, Kodansha Ltd, Tokyo, 1980, **1**, 1210.
15. Yu. V. Maksimov, I. P. Suzdalev, M. V. Tsodikov, V. Ya. Kugel, O. V. Bukhtenko, E. V. Slivinskii, and J. A. Navio, *J. Mol. Catal. A (Chem.)*, 1996, **105**, 167.
16. P. S. Cook, L. S. Chuan, H. Q. Sheng, W. R. Jackson, and P. J. Cassidg, *Fuel*, 1988, **67**, 942.
17. M. V. Tsodikov, Yu. V. Maksimov, G. A. Teplyakova, and M. A. Perederii, *Khim. Tverd. Topliva [Chemistry of Solid Fuel]*, 1992, **3**, 46 (in Russian).

Received June 6, 1996;
in revised form July 17, 1996